PHYSICAL REVIEW C **100**, 011301(R) (2019)

Rapid Communications

Excitations of the magic $N = 50$ neutron-core revealed in ^{81}Ga

J. Dudouet,[1,2,*] A. Lemasson,[3] G. Maquart,[1] F. Nowacki,[4] D. Verney,[5] M. Rejmund,[3] G. Duchêne,[4] O. Stezowski,[1] E. Clément,[3] C. Michelagnoli,[3] A. Korichi,[2,3] C. Andreoiu,[6] A. Astier,[2] G. de Angelis,[7] G. de France,[3] C. Delafosse,[5] I. Deloncle,[2] F. Didierjean,[4] Z. Dombradi,[8] C. Ducoin,[1] A. Gadea,[9] A. Gottardo,[5] D. Guinet,[1] B. Jacquot,[3] P. Jones,[10] T. Konstantinopoulos,[2] I. Kuti,[8] F. Le Blanc,[4] S. M. Lenzi,[11,12] G. Li,[13] R. Lozeva,[4,2] B. Million,[14] D. R. Napoli,[7] A. Navin,[3] R. M. Pérez-Vidal,[9] C. M. Petrache,[2] D. Ralet,[15,2] M. Ramdhane,[16] N. Redon,[1] C. Schmitt,[3] and D. Sohler[8]

[1]*Université Lyon 1, CNRS/IN2P3, IPN-Lyon, F-69622, Villeurbanne, France*

[2]*CSNSM, Université Paris-Sud, CNRS/IN2P3, Université Paris-Saclay, 91405 Orsay, France*

[3]*GANIL, CEA/DRF-CNRS/IN2P3, BP 55027, 14076 Caen cedex 5, France*

[4]*Université de Strasbourg, CNRS, IPHC UMR 7178, F-67000 Strasbourg, France*

[5]*Institut de Physique Nucléaire, IN2P3-CNRS, Université Paris-Sud, Université Paris Saclay, 91406 Orsay Cedex, France*

[6]*Department of Chemistry, Simon Fraser University, Burnaby, British Columbia, Canada*

[7]*INFN, Laboratori Nazionali di Legnaro, Via Romea 4, I-35020 Legnaro, Italy*

[8]*Institute for Nuclear Research of the Hungarian Academy of Sciences, Pf.51, H-4001, Debrecen, Hungary*

[9]*Instituto de Física Corpuscular, CSIC-Universitat de València, E-46980 Valencia, Spain*

[10]*iThemba LABS, National Research Foundation, P.O.Box 722, Somerset West,7129 South Africa*

[11]*INFN Sezione di Padova, I-35131 Padova, Italy*

[12]*Dipartimento di Fisica e Astronomia dell'Università di Padova, I-35131 Padova, Italy*

[13]*GSI, Helmholtzzentrum für Schwerionenforschung GmbH, D-64291 Darmstadt, Germany*

[14]*INFN, Sezione di Milano, Milano, Italy*

[15]*Institut für Kernphysik, Technische Universität Darmstadt, D-64289 Darmstadt, Germany*

[16]*LPSC, Université Grenoble-Alpes, CNRS/IN2P3, 38026 Grenoble Cedex, France*

(Received 11 January 2019; revised manuscript received 30 April 2019; published 12 July 2019)

The high-spin states of the neutron-rich ^{81}Ga, with three valence protons outside a ^{78}Ni core, were measured. The measurement involved prompt γ-ray spectroscopy of fission fragments isotopically identified using the combination of the variable mode spectrometer (VAMOS++) and the advanced gamma tracking array (AGATA). The new γ-ray transitions, observed in coincidence with ^{81}Ga ions, and the corresponding level scheme do not confirm the high-spin levels reported earlier. The newly observed high-spin states in ^{81}Ga are interpreted using the results of state-of-the-art large-scale shell model (LSSM) calculations. The lower excitation energy levels are understood as resulting from the recoupling of three valence protons to the closed doubly magic core, while the highest excitation energy levels correspond to excitations of the magic $N = 50$ neutron core. These results support the doubly magic character of ^{78}Ni and the persistence of the $N = 50$ shell closure but also highlight the presence of strong proton-neutron correlations associated with the promotion of neutrons across the magic $N = 50$ shell gap, only few nucleons away from ^{78}Ni.

DOI: 10.1103/PhysRevC.100.011301

Doubly magic nuclei with shell closures [1,2] and their neighbors serve as cornerstones to understanding and microscopically describing the atomic nucleus [3]. Intense efforts have been dedicated to gathering detailed experimental information about nuclear properties in the regions of shell closures to constrain the description of the nuclear force in terms of effective nucleon-nucleon residual interaction [4,5]. Recent results of studies in exotic nuclei far from stability, with a large imbalance of protons and neutrons, evidenced that classical shell closures can disappear due to the shell migration phenomena [3,6,7] or that the strong binding energy gain resulting from collective correlations can overcome the energy gap of shell closures [5,8–11].

The nickel isotopic chain, with three experimentally accessible isotopes characterized by classical magic numbers ($Z = 28$ and $N = 20, 28, 50$), is a unique laboratory to study shell evolution phenomena. ^{78}Ni represents a frontier in this quest. The $Z = 28$ shell closure is well known for exhibiting a strong magic behavior. However, in Cu isotopes ($Z = 29$), the lowering of the $1f_{5/2}$ orbital induces a reduction of $\approx$2 MeV of the $Z = 28$ shell gap between $N = 40$ and $N = 50$ [12]. Further, many efforts have been devoted to the characterization of the $N = 50$ shell gap [13–20] and support a possible weakening of the gap at $Z = 32$ [21,22], whereas a persistent $N = 50$ gap has been suggested at $Z = 30$ [19]. The experimental efforts in this region have been focused on the study of low-energy states, providing crucial information on the valence single-particle energies and the relevant interaction [21,21–26]. The γ-ray spectroscopy of ^{78}Ni was

*Corresponding author: jeremie.dudouet@csnsm.in2p3.fr

recently reported, providing the first experimental evidence of its doubly magic character [27]. Further indirect experimental evidences of the robustness of ^{78}Ni doubly magic core were reported from β-decay half-lives in the region [28], from masses of Cu isotopes [29], and from the study of low-lying excited states of ^{79}Cu [20] and ^{80}Zn [19].

Recent advances in the theoretical description of this region of the nuclear chart [11,30,31] gave different insights. In general it is agreed that ^{78}Ni itself manifests a doubly magic character. However, in Ref. [11] the sudden emergence of collective states and their coexistence with the spherical states are predicted. These spherical states arise mainly from one particle-hole (1 p-h) excitations across the magic shell gaps ($Z = 28$ and $N = 50$). Collective states arise from multiple particle-hole excitations, giving rise to a deformed collective band, providing a striking example of shape coexistence. This phenomenon is predicted to act as a portal to a new island of inversion for nuclei with $Z < 28$, where the intruder configurations, based on multiple particle-hole excitations, are predicted to dominate the ground and yrast states. While these very exotic nuclei remain inaccessible experimentally today, $N = 50$ isotones above ^{78}Ni, with few valence protons, can benchmark theoretical models and thereby elucidate the physics mechanisms behind the nuclear structure, and its evolution, toward ^{78}Ni.

Here, we report on spectroscopy of the $N = 50$ isotone ^{81}Ga, with three protons outside the ^{78}Ni core. We especially focus on the case of new high-spin states, which involve the coupling of valence protons to core excitations. The shell gap has been relatively well studied through the ground-state properties which themselves do not involve dominant single particle-hole contributions. The excited states of $N = 50$ isotones provide complementary insight into the coupling of single particle-hole configurations with valence protons where the particle-hole configurations are intimately related to the properties of the $N = 50$ shell gap. These new data offer a well-suited benchmark for state-of-the-art theoretical models such as the large-scale shell model (LSSM) [11], which has been found to successfully reproduce the experimental measurements on dipole and quadrupole moments [32] and masses [29] in Cu isotopes, as well as low-lying states in Zn isotopes [33].

Ground and excited states in ^{81}Ga were previously studied by means of collinear laser spectroscopy [34], β-decay [16,35,36], fast timing [36], and multinucleon transfer reactions [18].

The new high-spin states in ^{81}Ga have been observed using prompt γ-ray spectroscopy of isotopically identified fission fragments using the combination of the large-acceptance magnetic spectrometer VAMOS++ [37,38] and the AGATA advanced γ-ray tracking array [39–41]. ^{81}Ga nuclei were produced at GANIL using a ^{238}U beam at 6.2 MeV/u and a 10-micron-thick ^{9}Be target. VAMOS++ was used to obtain an event-by-event determination of the mass number (A) and atomic number (Z) of the detected fragments [42]. γ rays emitted at the target position were detected with AGATA, composed of eight triple clusters, placed in compact configuration (13.3 cm from the target). The positions of the

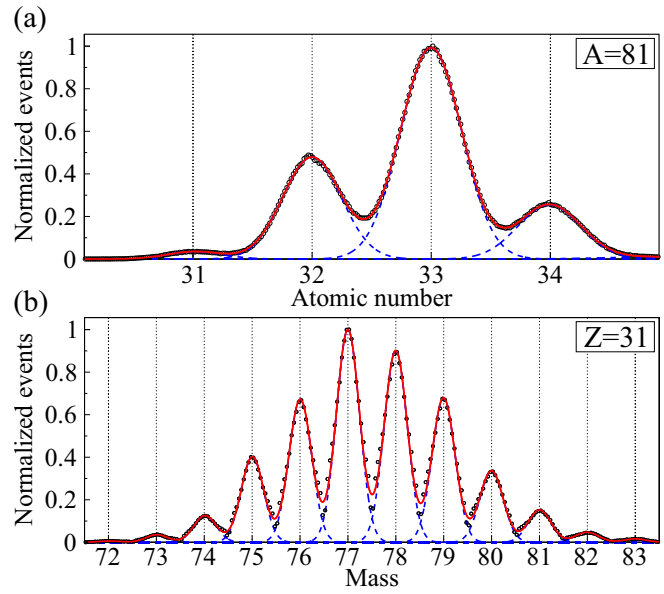

FIG. 1. (Top) Normalized atomic number distribution for $A = 81$ isotopes. (Bottom) Normalized mass distribution for $Z = 31$ isotopes. The continuous red and dotted blue lines represent, respectively, the fit of the total distributions and individual mass and atomic charge contributions.

γ-ray interaction points were determined using a pulse-shape analysis method [43,44]. The γ-ray path in the detector was reconstructed using a tracking algorithm [45] to obtain the total γ-ray energy along with the precise position of its first interaction. The combination of the measurement of the velocity vector of the fission fragments using VAMOS++ and the determination of the position of the first interaction of the γ ray in AGATA allowed us to apply a precise event-by-event Doppler correction. A γ-ray energy resolution of 5 keV (FWHM) has been obtained at 1.2 MeV for a v/c of $\approx$0.1. More experimental details are given in Ref. [46].

Figure 1 shows the atomic charge and mass distributions for $A = 81$ and $Z = 31$ isotopes, observed in coincidence with γ rays in this experiment. The figure illustrates the quality of the isotopic identification and the relative production yields. The analysis procedure and isotopic selectivity were systematically checked on the dataset and already demonstrated for the ^{96}Kr nucleus [46]. In particular, a very good agreement was found with the γ-ray transitions reported in the literature for ^{83}As and ^{82}Ge [18,47,48]. Further, it was found in these $N = 50$ isotones that the yrast states are dominantly populated in the presently used reaction mechanism. The tracked Doppler corrected γ-ray spectra obtained in coincidence with ^{81}Ga are shown in Fig. 2 and the energies and intensities of the six transitions observed in this work are summarized in Table I. The 350.6 keV transition was already reported in previous β-decay measurements and assigned to the depopulation of the first $3/2^-$ state [16,35,36]. The 1340.7 and 611.5 keV transitions were recently reported in Ref. [36]. The present work does not confirm any of the previously reported transitions from Ref. [18] where collisions of an ^{82}Se beam

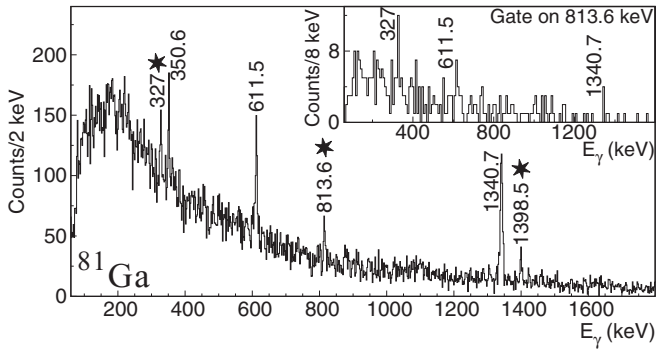

FIG. 2. Tracked Doppler corrected γ-ray spectrum measured in coincidence with the isotopically identified ^{81}Ga. Known γ-ray transition energies are labeled and newly reported transitions are marked with star symbols. The inset shows the γ-γ coincidence gated on the 813.6 keV transition in ^{81}Ga.

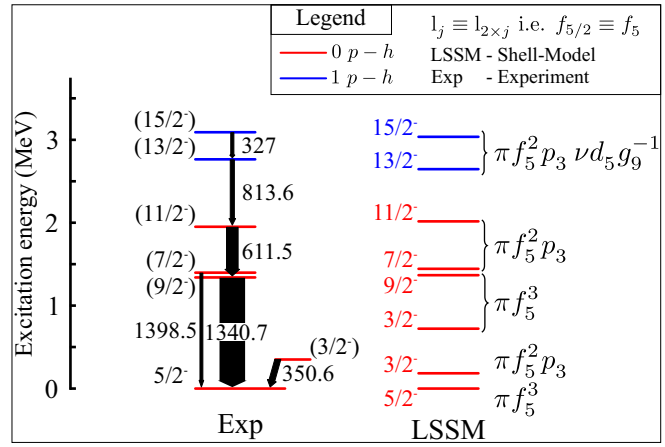

FIG. 3. Experimental level scheme observed in the present work (left) and theoretical level scheme (right) of ^{81}Ga. Levels marked with red (blue) correspond to dominant contributions from 0 p-h (1 p-h) excitations of the ^{78}Ni core.

with a ^{238}U target were used. In Ref. [18], the reported γ-ray spectrum of ^{81}Ga has, however, very limited statistics.

The inset of Fig. 2 shows the γ-γ coincidence spectrum gated on the 813.6 keV transition. The 327.0, 611.5, and 1340.7 keV transitions were observed in coincidence. The level scheme, constructed on the basis of γ-γ coincidences and relative intensities of observed transitions, is shown in the left side of Fig. 3. The tentative spin and parity assignments were made assuming a dominant population of the yrast states in fission reactions. The right side of Fig. 3 shows the results of LSSM calculations using the PFSDG-U interaction [11]. The valence space corresponds to the pf orbitals for protons and sdg orbitals for neutrons, using an inert core of ^{60}Ca. More details on this theoretical framework can be found in Ref. [11]. The relevant dominant configurations of the excited states, as predicted by the model, are also shown in Fig. 3.

The three protons outside the $Z = 28$ and $N = 50$ doubly magic core occupy the low-lying valence orbitals ($1f_{5/2}$, $2p_{3/2}$, and $2p_{1/2}$). In this case, the negative parity states with spin values up to $J^\pi = 5/2^-$ without pair breaking, and up to $J^\pi = 11/2^-$ with one broken proton pair, can be built. Therefore, the low-lying excited states until $J^\pi = 11/2^-$ can be interpreted as mainly due to the coupling of the three valence protons. The states with larger spin require the excitation of particles across the magic gaps from the ^{78}Ni inert core. In the $J^\pi = 13/2^-$ and $J^\pi = 15/2^-$ levels, the coupling of valence protons (configuration $\pi f_{5/2}^2 p_{3/2}$) with 1 p-h excitation (configuration $\nu d_{5/2} g_{9/2}^{-1}$) becomes dominant. A very good agreement between the experimental level energies and the calculations can be seen in Fig. 3. The calculations predict that the newly reported states $J^\pi = 13/2^-$ and $J^\pi = 15/2^-$ are associated with p-h excitations, dominantly of neutrons across the $N = 50$ gap, resulting from large proton-neutron correlations.

Excited states arising from the coupling of valence protons to core excited states carry information on the magnitude of the $N = 50$ shell gap. The amplitude of the shell gap Δ_n, that includes correlations present in the ground state, can be obtained from binding energies and can be expressed as follows:

$$\Delta_n = \mathrm{BE}(Z, 51) + \mathrm{BE}(Z, 49) - 2 \times \mathrm{BE}(Z, 50), \quad (1)$$

where $\mathrm{BE}(Z, N)$ represents the binding energy of nucleus ${}^{A}_{Z}X_N$. Figure 4 shows the shell gap (Δ_n) using the experimental masses (solid lines) [29,49] as a function of the proton number for $N = 50$ isotones along with known and newly measured $J^\pi = 5^+, 6^+$ and $13/2^-, 15/2^-$ excited states. The dotted lines for $Z = 29$ use extrapolated masses of ^{80}Cu from mass evaluation [49]. In addition, the predictions for Δ_n from LSSM calculations are also shown for $28 \leqslant Z \leqslant 34$. It can be seen that the experimental Δ_n follow a continuous reduction from $Z = 34$ till $Z = 31$. For $30 < Z < 34$, the measured excited states are well correlated with the experimental Δ_n. The correlation between experimental Δ_n and the excitation energies suggests that these states involve neutron p-h excitation across the $N = 50$ shell gap, though for $Z > 32$ these states could be formed by recoupling of the valence protons only. Note, however, that $J^\pi = 15/2^-$ states must involve other excitations than protons in $f_{5/2}$, $p_{3/2}$, $p_{1/2}$. While the 5^+ and 6^+ states in ^{82}Ge and ^{84}Se can result from the recoupling of valence protons only, particle-hole excitation across the $N = 50$ gap is required

TABLE I. γ-ray transition energies (E_γ), associated initial and final level energies and efficiency corrected intensities relative to the 1340.7 keV transition (I_γ) in the ^{81}Ga nucleus.

E_γ (keV)	E_i (keV)	E_f (keV)	I_γ
1340.7(4)	1340.7(4)	0	100(20)
611.5(5)	1952.2(7)	1340.7(4)	52(10)
813.6(8)	2765.8(11)	1952.2(7)	24(6)
350.6(3)	350.6(3)	0	19(5)
327.0(2)	3092.8(23)	2765.8(11)	18(4)
1398.5(7)	1398.5(7)	0	17(5)

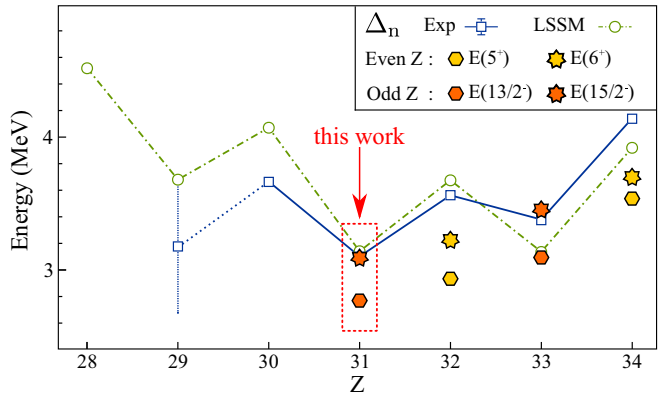

FIG. 4. Comparison between the Δ_n shell gap at $N = 50$ and the energy of core-excited states in $N = 50$ isotones. Solid line: Δ_n from binding energies [29,49,50]. Dashed-dotted line: Δ_n from LSSM calculations. Symbols: excitation energy of core-excited states [48]. The dotted line represents Δ_n using extrapolated mass for ^{80}Cu (see text).

to form these states in ^{80}Zn. The high spin states in ^{81}Ga and ^{80}Zn give therefore a unique opportunity to reveal the coupling of valence protons to core excited states. Further, the calculated and experimental Δ_n are in good agreement, supporting the quality of the calculation. The calculated Δ_n show a rapid increase toward $Z = 28$, indicating a robust doubly closed shell ^{78}Ni.

Further insight into the structure of the excited states of ^{81}Ga and their relation to the ^{78}Ni core can be obtained by studying the different decompositions of the calculated wave functions. Figure 5 shows the prediction from LSSM calculations for the excited states and configurations for ^{78}Ni and ^{81}Ga. The wave function can be decomposed in terms of proton (red) and neutron (blue) type p-h core excitations. This decomposition is represented for each level by a colored bar (the full level width is equivalent to 100%). The fraction of the wave function without any p-h contribution (i.e., inert core) is represented in white. Further, the histograms show the distribution in terms of the total number of particle-hole excitations of the inert core ($n^{\nu}_{\text{p-h}} + n^{\pi}_{\text{p-h}}$) contributing to the states of interest. For ^{81}Ga, states up to $11/2^-$ exhibit the structure of three valence protons coupled to the ground state of ^{78}Ni. The dominance of the closed doubly magic inert core (in white) can be seen. The situation changes for states with $J^{\pi} > 11/2^-$ where the neutron-type 1 p-h configurations dominate (≈85%).

Similar decompositions of the wave functions can be obtained for ^{78}Ni. As reported in Ref. [11], a coexistence between spherical (left) and collective (right) states in ^{78}Ni is calculated and shown in Fig. 5. The difference in the distribution of the number of p-h excitations between spherical and deformed states is striking: the configurations of the former are dominated by 1 p-h excitations (up to 50% of the wave function in the 6^+ state) while the configurations of deformed states consist of 4 p-h or more (≈90% of the wave function). It can be seen from Fig. 5 that the ground state of ^{78}Ni is predicted to be spherical, mainly doubly closed shell with small contribution of neutron and proton type p-h excitations of the core. In contrast, excited states are built on both proton and neutron type p-h excitations, having nearly equivalent contributions.

The comparison between the LSSM results for ^{78}Ni and ^{81}Ga leads to the following observations. In the ground state of ^{78}Ni, the relative importance of proton and neutron p-h excitations is balanced, due to relatively equal $Z = 28$ and $N = 50$ gap sizes, whereas for ^{81}Ga having valence protons, the Pauli principle rapidly hinders proton excitations, favoring neutron type p-h excitations. Second, the distributions of the total number of p-h excitations for states with $J^{\pi} > 11/2^-$ have some similarity to those of spherical excited states in ^{78}Ni. Note, however, that (i) the $n^{\nu}_{\text{p-h}} + n^{\pi}_{\text{p-h}}$ distributions present slightly different shapes in ^{78}Ni and in ^{81}Ga; (ii) the contribution of proton-type p-h excitations is strongly suppressed in ^{81}Ga. Consequently the high spins $J^{\pi} = 13/2^-, 15/2^-$, where the valence protons are coupled to the core excitations, exhibit a sensitivity to the $N = 50$ gap. This observation highlights the dominant role of valence protons coupling with neutron type p-h excitations in the nucleus only three protons above ^{78}Ni. These predictions, in line with the observation of a minimum of the effective $N = 50$ gap at $Z = 31$ in the direct vicinity of the $Z = 28$ shell closure, highlight a rapid development of the correlations in this region. A feature which is presumably consistent with the recently reported large quadrupole strength in ^{84}Ge [51], where only four protons and two neutrons are added to ^{78}Ni. Further experimental and theoretical investigations are therefore needed for interpretation of the complex phenomena arising in the vicinity of ^{78}Ni.

In conclusion, high spin states in ^{81}Ga have been reported using prompt γ-ray spectroscopy of isotopically identified fission fragments. The predictions of the state-of-the-art LSSM calculations are in very good agreement with the experimentally measured levels, illustrating the reliability of the model in this region. The calculations suggest that the newly reported states are built on configurations with the three valence protons coupled to the ^{78}Ni core and highlight the dominant role of valence protons coupling with neutron-type p-h excitations in the description of high-spin states. The excited states, at relatively low energy, follow the shell gap obtained from mass measurements confirming their relation with neutron p-h excitations across the $N = 50$ gap and illustrating the role of large proton-neutron correlations. This result supports the doubly magic character of ^{78}Ni and its persistence for $N = 50$ isotones for $Z > 28$ in contrast to the sudden development of collectivity for $Z < 28$, predicted in the same shell-model framework of Ref. [11].

In the future, similar studies of core-excited configurations in $N = 50$ isotones with one and two valence protons (^{79}Cu and ^{80}Zn) will complete a coherent picture of the evolution of core excitation of the doubly magic ^{78}Ni in the presence of valence protons and thus providing strong constraints on the effective interaction in this region. In particular, core-excited state energies will provide a stringent test of the increasing shell gap observed in ^{80}Zn and predicted in ^{79}Cu.

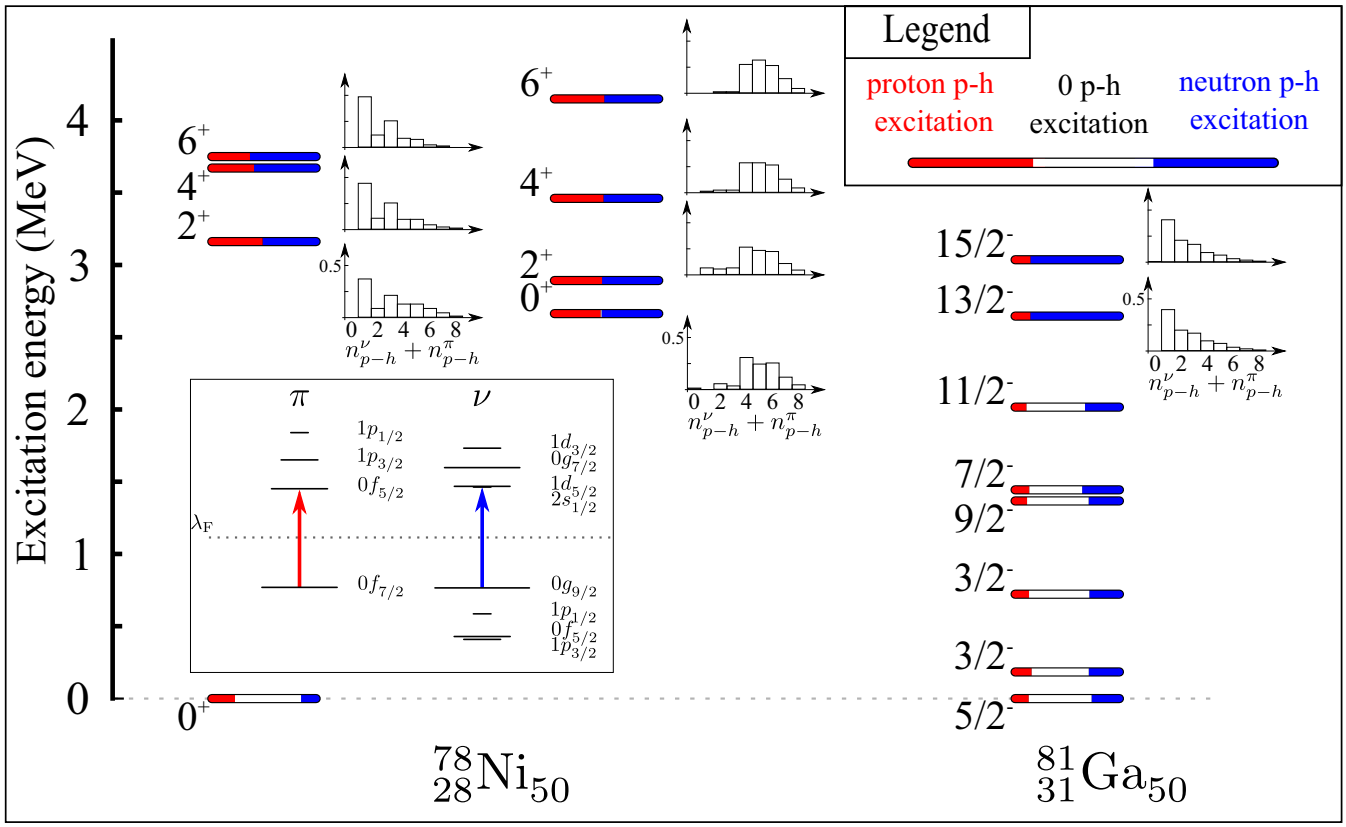

FIG. 5. Theoretical predictions for excitation energies and decomposition of the wave functions for states in ^{78}Ni [11] and ^{81}Ga (this work). For ^{78}Ni the spherical (left) and collective (right) states are shown. The histograms represent the distribution of total number of particle-hole excitations of the inert core ($n^{\nu}_{\text{p-h}} + n^{\pi}_{\text{p-h}}$) contributing to the state. The contribution of the excitations of the inert core due to the protons (red) and neutrons (blue) is represented in color in terms of probability in each level (the length of the color bar is normalized to 100% for each state), the white area corresponds to a closed inert core configuration. The relevant single-particle proton and neutron states are also shown.

We acknowledge the important technical contributions of J. Goupil, G. Fremont, L. Ménager, J. Ropert, C. Spitaels, and the GANIL accelerator staff. This work was supported by the BMBF under No. 05P09RDFN4 and No. 05P12RDFN8, and by the LOEWE center HIC for FAIR. D.R. was partially supported by the P2IO Excellence Laboratory. D.S. acknowledges support under Project No. GANOP-2.3.3-15-2016-00034. A.G and R.P were partially supported by Ministry of Science, Spain, under the Grants FPA2017-84756-C4 and SEV-2014-0398, and by the EU FEDER funds. P.J. acknowledges support from National Research Foundation of South Africa (90741). Z.D., I.K. and D.S. acknowledge support of Hungarian National Research and Innovation Office (NKFIH) by No. K128947, PD124717, and the support under project GINOP-2.3.3-15-2016-00034. The authors also acknowledge support from the European Union seventh framework through ENSAR, Contract No. 262010.

[1] M. Goeppert-Mayer, Phys. Rev. **74**, 235 (1948).
[2] M. Goeppert-Mayer, Phys. Rev. **75**, 1969 (1949).
[3] O. Sorlin and M. G. Porquet, Prog. Part. Nucl. Phys. **61**, 602 (2008).
[4] J. P. Schiffer and W. W. True, Rev. Mod. Phys. **48**, 191 (1976).
[5] E. Caurier, G. Martínez-Pinedo, F. Nowacki, A. Poves, and A. P. Zuker, Rev. Mod. Phys. **77**, 427 (2005).
[6] T. Otsuka, Physica Scripta **152**, 014007 (2013).
[7] D. Steppenbeck *et al.*, Nature **502**, 207 (2013).
[8] E. K. Warburton, J. A. Becker, and B. A. Brown, Phys. Rev. C **41**, 1147 (1990).
[9] K. Wimmer *et al.*, Phys. Rev. Lett. **105**, 252501 (2010).
[10] E. Caurier, F. Nowacki, and A. Poves, Phys. Rev. C **90**, 014302 (2014).
[11] F. Nowacki, A. Poves, E. Caurier, and B. Bounthong, Phys. Rev. Lett. **117**, 272501 (2016).
[12] E. Sahin *et al.*, Phys. Rev. Lett. **118**, 242502 (2017).
[13] Y. H. Zhang *et al.*, Phys. Rev. C **70**, 024301 (2004).
[14] A. Prévost *et al.*, Eur. Phys. J. A **22**, 391 (2004).
[15] M. G. Porquet *et al.*, Eur. Phys. J. A **39**, 295 (2009).
[16] S. Padgett *et al.*, Phys. Rev. C **82**, 064314 (2010).
[17] M.-G. Porquet and O. Sorlin, Phys. Rev. C **85**, 014307 (2012).
[18] E. Sahin *et al.*, Nucl. Phys. A **893**, 1 (2012).
[19] Y. Shiga *et al.*, Phys. Rev. C **93**, 024320 (2016).

[20] L. Olivier *et al.*, Phys. Rev. Lett. **119**, 192501 (2017).
[21] J. Hakala *et al.*, Phys. Rev. Lett. **101**, 052502 (2008).
[22] A. Gottardo *et al.*, Phys. Rev. Lett. **116**, 182501 (2016).
[23] J. M. Daugas *et al.*, Phys. Lett. B **476**, 213 (2000).
[24] P. T. Hosmer *et al.*, Phys. Rev. Lett. **94**, 112501 (2005).
[25] C. Mazzocchi *et al.*, Phys. Lett. B **622**, 45 (2005).
[26] M. M. Rajabali *et al.*, Phys. Rev. C **85**, 034326 (2012).
[27] R. Taniuchi *et al.*, Nature **569**, 53 (2019).
[28] Z. Y. Xu *et al.*, Phys. Rev. Lett. **113**, 032505 (2014).
[29] A. Welker *et al.*, Phys. Rev. Lett. **119**, 192502 (2017).
[30] K. Sieja and F. Nowacki, Phys. Rev. C **85**, 051301(R) (2012).
[31] G. Hagen, G. R. Jansen, and T. Papenbrock, Phys. Rev. Lett. **117**, 172501 (2016).
[32] R. P. de Groote *et al.*, Phys. Rev. C **96**, 041302(R) (2017).
[33] C. M. Shand *et al.*, Phys. Lett. B **773**, 492 (2017).
[34] B. Cheal *et al.*, Phys. Rev. Lett. **104**, 252502 (2010).
[35] D. Verney *et al.* (PARRNe Collaboration), Phys. Rev. C **76**, 054312 (2007).
[36] V. Paziy, Ph.D. thesis, Universidad Complutense de Madrid, 2017.
[37] M. Rejmund *et al.*, Nucl. Instrum. Methods Phys. Res., Sect. A **646**, 184 (2011).
[38] M. Vandebrouck *et al.*, Nucl. Instrum. Methods Phys. Res., Sect. A **812**, 112 (2016).
[39] E. Clément *et al.*, Nucl. Instrum. Methods Phys. Res., Sect. A **855**, 1 (2017).
[40] A. Gadea *et al.*, Nucl. Instrum. Methods Phys. Res., Sect. A **654**, 88 (2011).
[41] S. Akkoyun *et al.*, Nucl. Instrum. Methods Phys. Res., Sect. A **668**, 26 (2012).
[42] A. Navin *et al.*, Phys. Lett. B **728**, 136 (2014).
[43] B. Bruyneel, B. Birkenbach, and P. Reiter, Eur. Phys. J. A **52**, 70 (2016).
[44] R. Venturelli and D. Bazzacco, LNL Annual Report 2004 (unpublished).
[45] A. Lopez-Martens *et al.*, Nucl. Instrum. Methods Phys. Res., Sect. A **533**, 454 (2004).
[46] J. Dudouet *et al.*, Phys. Rev. Lett. **118**, 162501 (2017).
[47] T. Rząca-Urban, W. Urban, J. L. Durell, A. G. Smith, and I. Ahmad, Phys. Rev. C **76**, 027302 (2007).
[48] ENSDF: Evaluated Nuclear Structure Data File, https://www.nndc.bnl.gov/ensdf/.
[49] M. Wang *et al.*, Chin. Phys. C **41**, 030003 (2017).
[50] R. N. Wolf *et al.*, Phys. Rev. Lett. **110**, 041101 (2013).
[51] C. Delafosse *et al.*, Phys. Rev. Lett. **121**, 192502 (2018).